Effects of solar irradiance on the upper ionosphere and oxygen ion escape at Mars. MAVEN observations

E. Dubinin,[1], M. Fraenz[1], M. Pätzold[2], J. McFadden[3], P. R. Mahaffy[4], F. Eparvier[5], J. S. Halekas[6], J. E. P. Connerney[4], D. Brain[5], B. M. Jakosky[5], O. Vaisberg[7], L. Zelenyi[7]

Corresponding author: E. Dubinin, Justus-Von-Liebig Weg, 3, Max-Planck-Institute for Solar System Research, 37077, Göttingen, Germany. (dubinin@mps.mpg.de)

[1]Max-Planck-Institute for Solar System Research, Göttingen, Germany.

[2]Rheinisches Institut fuer Umweltforschung, Abteilung Planetforschung, Cologne, Germany.

[3]Space Sciences Laboratory, U.C. Berkeley, Berkeley, CA, USA.

[4]NASA Goddard Space Flight Center, Maryland, USA.

This article has been accepted for publication and undergone full peer review but has not been through the copyediting, typesetting, pagination and proofreading process, which may lead to differences between this version and the Version of Record. Please cite this article as doi: 10.1002/2017JA024126

Abstract. We present multi-instrument observations of the effects of solar irradiance on the upper Martian ionosphere and escape fluxes based on the MAVEN data from November 2014 to February 2016. It is shown that fluxes of oxygen ions with $E > 30$ eV both inside and outside of the Martian magnetosphere are nonsensitive to EUV variations. In contrast, the fluxes of ions with lower energies extracted from the upper ionosphere increase with solar irradiance. Such an enhancement is nonlinear with the EUV variations and exhibits a growth by almost one order of magnitude when the EUV (0.1-50 nm) radiation increases to $\geq$ 0.1 W/m^2 implying an enhancement of total ion losses of the low-energy component to $\sim$ $1.8 \cdot 10^{25}$s^{-1}. The flow of cold ions in the near Mars tail occurs very asymmetrical shifting in the direction opposite to the direction of the the solar wind motional electric field. Fluxes of the low-energy (E $\leq$ 30 eV) ion component are also nonsensitive to the variations in solar wind dynamic pressure.

[5]Laboratory for Atmospheric and Space Physics, Univ. of Colorado, Boulder, CO, USA.

[6]Department of Physics and Astronomy, University of Iowa, Iowa City, Iowa, USA.

[7]Institute of Space Research, Moscow, Russia.

1. Introduction

The absence of a global magnetic field at Mars leads to the direct interaction of solar wind with its atmosphere/ionosphere. This type of interaction results in significant atmospheric losses (see e.g. *Vaisberg*, 1976, *Lundin et al.,* 1989, 2008a, *Barabash et al.,* 2007, *Dubinin et al.,* 2011, *Nilsson et al.,* 2011, *Fraenz et al.,* 2010, 2015, *Jakosky et al.,* 2015a, *Brain et al.,* 2015, *Dong et al.,* 2015) that might be important for the evolution of the Martian atmosphere and its water inventory. However, atmospheric losses in the present epoch are not sufficient to explain the dehydration of Mars. To estimate losses forced by the solar wind in past epochs when solar wind was stronger and solar irradiance was higher we need to know how the ionosphere of Mars and escape fluxes depend on variations of solar wind and solar EUV flux in the current epoch. Here we will focus on effects related to variations in the EUV flux which is an important energy supplier for the Martian ionosphere - the main reservoir for ion escape forced by solar wind.

Previous studies of this problem used the ASPERA-3 measurements on Mars Expess (MEX) and different proxies for solar EUV flux (*Lundin et al.* 2008b, *Nilsson et al.* 2010). *Lundin et al.* (2008b) have used the sensitivity of the Neutral Particle Imager (NPI) of the ASPERA-3 experiment onboard Mars Express to Lyman-α as a proxy of solar EUV fluxes. These authors have studied the response of ion escape to variations in the noise background of NPI based on 42 orbits selected from a 17 month period from December 2004 to June 2006 and have found that a decrease in the EUV flux by a factor of 2.5 leads to a decrease of outflow of ions with $E \leq 800$ eV also by a factor of 2.5. On the other hand, analyzing the ASPERA-3 data from May 2004 to November 2005 and using

as a proxy the solar EUV flux at Earth scaled and shifted to Mars, *Nilsson et al.* (2010) did not find any clear correlation between the solar EUV flux and the ion escape rate. A relationship between ion losses measured by ASPERA-3 and EUV flux was also studied by *Lundin et al.* (2013), *Ramstad et al.* (2015) and *Dubinin et al.* (2017). *Lundin et al.* (2013) have observed a high correlation of average and median tail fluxes of heavy ions (O^+, O_2^+) with $E \leq$300 eV, derived from the MEX observations carried out from June 2007 to January 2013. Making the regression analysis the authors have found the power law dependence between the ion flux and the solar activity proxy $F10.7$ ($F_{ion} \sim F10.7^{0.88}$). *Ramstad et al.* (2015) have studied the effect of EUV on ion escape 'freezing' the solar wind parameters. Authors did not separate fluxes of the low and high-energy ions and have found increase by a factor of two in the total ion escape between low and high EUV for similar conditions in the solar wind. *Dubinin et al.* (2017) have found that a clear positive correlation between oxygen ion losses and solar irradiance exists only for fluxes of low-energy ions. On the other hand, the measurements of these ions ($10 \leq E_i/q \leq 50$) eV by ASPERA-3 have serious constraints because of the narrow field-of-view (4^o x 360^o) of the instrument and therefore can provide only a qualitative picture (*Dubinin et al.*, 2017).

Recently, *Dong et al.* (2017) have investigated the seasonal variability of the ion escape ($E_i \geq$6 eV) in response to the solar extreme ultraviolet (EUV) flux based on the MAVEN observations. Authors constrain the solar wind dynamic pressure and interplanetary magnetic field strength and compare the ion escape rates through the tail in different EUV conditions. *Dong et al.* (2017) have found that the total escape rate of ions with $E_i \geq 6$ eV increases at 1.5 times when the EUV irradiance increases by almost the same factor.

The measurements made by the MAVEN spacecraft provide for the first time the opportunity to study these processes with simultaneous monitoring of the ionospheric variations, planetary ion fluxes and solar wind and solar irradiance in more detail. The ion sensor STATIC on MAVEN measuring the fluxes of low-energy ions is able to detect ions with $E_i \geq 0.1$ eV in a wide field-of-view (90^o x 360^o) (*McFadden et al.,* 2015). Since EUV emissions are temporary and spatially dependent on solar rotation and flare activity the in-situ monitoring of EUV fluxes at Mars allows us to study the variability in the coupling between the Sun and the Martian ionosphere more truthfully. The instrument payload on MAVEN also allow measuring of thermal ionospheric ion species and monitor the solar wind conditions (*Jakosky et al.,* 2015b).

2. Instrumentation

The MAVEN spacecraft arrived at Mars in September 2014 to study the processes in the upper atmosphere/ionosphere and its interaction with solar wind (*Jakosky et al.,* 2015a, b). MAVEN was inserted into an elliptical orbit with periapsis and apoapsis of 150 km and 6200 km, respectively, and with a period of 4.5 hours. The spacecraft carries 9 sensors which measure the input fluxes of solar wind and solar irradiance and monitor the response of the Martian atmosphere/exosphere and ionosphere on these driving inputs (*Jakosky et al.,* 2015b). In this paper we used the data from 5 instruments to study effects of the variability in the solar irradiance on the structure of the upper ionosphere and ion losses from November 1, 2014 to February 15, 2016.

The Extreme Ultraviolet Monitor on the MAVEN spacecraft consists of three broadband radiometers in the ranges 0.1-7 nm, 17-22 nm and 121-122 nm providing us information about variability of soft X-rays and EUV fluxes at Mars (*Eparvier et al.,* 2015). Emissions

in the ranges of 0.1-7 nm and 17-22 nm originating in the hot and cooler solar corona, respectively, are used to monitor solar flares. Emissions in the range 121-122 nm due to the HI Lyman-α line are used as a proxy of long-term variations in solar irradiance. These data were also used to generate the full EUV spectrum at Mars combining the MAVEN measurements and the observations at Earth orbit on TIMED-SEE and SOLSTICE instruments interpolated to the Mars position at the time of the MAVEN measurements (L3 data product). In this study we were more interested in the long-term variations in the upper ionosphere and ionospheric losses and therefore used this product for the full spectral irradiance in the range of 0.1-50 nm.

The Neutral Gas and Ion Mass Spectrometer (NGIMS) on the MAVEN spacecraft measures the composition of the upper atmosphere and the ionosphere below 500 km (*Mahaffy et al.,* 2015). It consists of the dual ion source and the quadrupole mass analyzer operating in neutral and ion modes. The instrument operates collecting particles from the RAM direction. This narrow field-of-view of NGIMS ($\leq 2^o$) is maintained by the Actuated Payload Platform (APP). Here we use only the density of the main ionospheric species O_2^+ and O^+ retrieved in the ion mode of NGIMS.

Supra-Thermal And Thermal Ion Composition (STATIC) instrument also mounted on APP measures energy spectra of ion fluxes in the range of 0.1 eV-30 keV and the ion composition (*McFadden et al.,* 2015). It consists of a toroidal top hat electrostatic spectrometer with the electrostatic deflector at the entrance providing 360^o x 90^o field of view combined with time-of-flight velocity analyzer resolving the major H^+, He^{++}, He^+, O^+, O_2^+ and CO_2^+ ion species. The measurements allow a retrieval of the velocity distribution functions and their moments (density, velocity, temperature) for different ion species. The

measurements of the low-energy ions in the dense ionosphere and in the planetary wake are affected by the negative spacecraft potential. Therefore calculating the ion distribution functions we made corrections using the spacecraft potential. Corrections related to the spacecraft velocity were also applied. The instrument operates in different modes (RAM, Conic and Pickup) providing different data products with different mass, energy, angular and time resolution. In this study we used 'joined' products which have 32 energy steps, 4 deflector angles (elevation angles), 16 anodes (azimuth angles), 8 ion masses and 4 sec cadence to calculate the moments of the ion distribution functions.

The Solar Wind Ion Analyzer (SWIA) is a toroidal energy analyzer with electrostatic deflectors to provide a broad 90^o x 360^o field of view with a mechanical attenuator to enable a very high dynamic range (*Halekas et al.,* 2015). SWIA is monitoring solar wind providing high cadence (4 s) measurements of ion velocity distributions in the 30 eV to 25 keV energy range with 14.5 % energy resolution and 3.75^o x 4.5^o angular resolution in the sunward direction.

We also used the magnetic field data from two independent tri-axial fluxgate magnetometers (MAG) mounted on the booms of the MAVEN spacecraft (*Connerney et al.,* 2015).

3. Observations

There are different channels and energization processes through which the exospheric/ionospheric ions escape from Mars (*Dubinin et al.,* 2011) and therefore the response on solar wind/EUV variations in these channels might be also different. The MAVEN measurements allow easily to distinguish between these channels. Ions extracted from the extended hydrogen and hot oxygen exosphere and the external layers of the iono-

sphere move like test particles gaining energy by acceleration in the $-V$ x B electric field (*Dubinin et al.,* 2011, *Dong et al.,* 2015). These ions are accelerated to high energies filling mainly the region outside the induced Martian magnetosphere (the ion plume). Figure 1a shows a map of the energy corresponding to peak fluxes of oxygen ions in cylindrical projection with the nominal positions of the bow shock and the magnetosphere boundary. It is seen that O^+ ions gain the highest energies in the solar wind and magnetosheath. However, the major fraction ($\sim 80\%$, *Dong et al.,* 2015) of escape is carried by ions with lower energies which is confirmed by Figure 1b which depicts fluxes of O^+ ions in cylindrical coordinates. These ions are extracted from deeper ionospheric shells and behave like a fluid ("comet-like" outflow (*Lundin et al.,* 2008b)) occupying mainly the interior magnetosphere. In this paper we will focus mainly on this ion population.

3.1. Variations in the upper ionosphere and in the trans-terminator fluxes

The upper ionosphere is the main reservoir for ions which fill the Martian magnetosphere and therefore we address at first the question how does the upper ionosphere respond to variations in solar irradiance. Figures 2a and 2b show maps of the density of molecular and atomic oxygen ions measured by NGIMS at $70^o - 100^o$ solar zenith angles as function of the altitude and EUV flux. It is seen that for a fixed altitude the ion density generally increases with increase in the solar activity. The effect is well observed at altitudes above $\sim$ 200 km. The upper parts of these maps present the altitude profiles of the density of molecular and atomic oxygen ions for time intervals characterized by different solar irradiance. Red and blue lines show the density profiles of O_2^+ and O^+ ions at EUV = 0.09-0.1 W/m^2 and 0.05-0.06 W/m^2, respectively. With an increase of solar EUV flux by

approximately a factor of two, the ion density in the upper ionosphere increases by 1.5-2 times.

A similar dependence of the ion density on the EUV flux is observed at higher altitudes sampled by the STATIC measurements. Figure 2c and 2d show maps of the density measured by STATIC at SZA $= 70^o - 100^o$ and their altitude profiles at different levels of solar activity. The ion density increases with increase in solar radiation. With increase in altitude the effect of solar irradiance gradually diminishes. Note that the measurements made on MEX by the MARSIS instrument in the same range of the solar zenith angles also show a positive correlation of the total electron density with EUV fluxes but such an effect was observed at all sampled altitudes (≤ 1400 km) (*Dubinin et al.,* 2017). It might be that STATIC failed to detect the cold thermal ion component at high altitudes where the spacecraft potential is ≥ 0.

Figure 3 shows the dependence of the density of O^+ ions measured by STATIC at $SZA = 70 - 100^o$ and altitudes of 300-400 and 400-600 km on the EUV flux. The black and green lines depict the mean and median values, respectively. The standard deviations are also given. We observe a strong growth in the density at the highest EUV fluxes. Comparing again with the MEX measurements, which were carried for a much longer period, note that *Dubinin et al.* (2017) have found a linear relation between the Log (Density) and EUV flux.

Correspondingly, one may expect an increase of the trans-terminator flux of oxygen ions from day to night at higher solar activity. Figure 4 shows maps of the trans-terminator fluxes of O_2^+ and O^+ ions with energies $E \leq 30$ eV at different levels of solar irradiance. The choice of the upper energy $E = 30$ eV for fluxes of the low-energy ions will be discussed

later. The plots on the bottom of these maps depict the altitude profiles of the fluxes measured at EUV = 0.09-0.1 W/m^2 (red) and 0.05-0.06 W/m^2 (blue), respectively. It is observed that the trans-terminator ion flux increases with increase in solar irradiance at altitudes below $\sim$ 800 km and the difference in fluxes at lower altitudes can reach a factor of 5-6 while the EUV flux increases only in approximately two times. Figure 5 depicts variations of the mean values of the trans-terminator fluxes of O^+ and O_2^+ ions ($E \leq 30$ eV) measured at different altitudes with solar irradiance. Despite of large fluctuations in values a significant increase is obvious at EUV flux higher than 0.09 W/m^2. Ion fluxes of O^+ ions with $E > 30$ eV measured outside of the Martian magnetosphere do not reveal any relationship with solar irradiance. Note here that the values of these fluxes are very low because the averaging is done in cylindrical coordinates which ignore their focusing in the plume area.

3.2. Variations of fluxes in the tail

It is well known that ion fluxes in the Martian tail are unevenly distributed due to a focusing effect caused by ion acceleration by j x B forces. It is usually clearly seen by plotting the data in MSE coordinates (*Dubinin et al.,* 1996, 2011, *Dubinin and Fraenz,* 2015, *Barabash et al.,* 2007, *Dong et al.,* 2015) that allow to identify the plasma sheet of the induced magnetosphere. Here we use another set of variables to separate different tail regions. Figure 6 shows maps of fluxes of oxygen (O^+) ions in the $B_x - X$ coordinates, where B_x is the X_{MSO}-component of the magnetic field locally measured by the MAG instrument onboard MAVEN and X - is the s/c coordinate in the MSO reference frame. Top (bottom) panels compare fluxes of ions with $E > 30$ eV ($E \leq 30$ eV), respectively. A change of sign in the B_x-component corresponds to the crossing of the central current

sheet. This type of representation allows to avoid uncertainties related with the determination of the MSE coordinate system (see e.g. *Modolo et al.,* 2012) and flapping motions of the plasma sheet (*Dubinin et al.,* 2012). The enhancement of ion fluxes around the current sheet observed for ions with $E > 30$ eV is consistent with a plasma sheet crossing. The rest area corresponds to the tail lobes. It is seen that the low-energy ions ($E \leq 30$ eV) fill mainly the lobes.

The data were sorted by solar irradiance. A simple inspection of the color maps shows that fluxes of ions with $E > 30$ eV are almost nonsensitive to solar irradiance. In contrast, the fluxes of ions with lower energies exhibit a strong increase at the highest level of solar activity and begin to fill also the central part of the tail.

It is also seen that the tail region was not properly sampled near apoapsis at the period of high solar activity. That is why we can compare the values of fluxes only in the near Mars tail. The bottom parts of Figures 6b and Figure 6d contain the plots of ion fluxes at $-1.6R_m < X < -1.2R_m$ across the tail as a function of B_x for two different states of solar activity - 0.045-0.06 W/m^2 and 0.08-0.1 W/m^2). The solid and dotted lines are the mean and median values, respectively. Fluxes of ions with $E > 30$ eV remain almost the same with a change in the EUV flux. In contrast, fluxes of low energy ions reveal a clear dependence on solar EUV. We observe a significant enhancement by a factor of ~ 10 in fluxes during the periods when solar EUV flux increased up to 0.08-0.1 W/m^2.

Figure 7 summarizes the relationship between O^+ ion fluxes measured in the different energy intervals in the tail (-10 nT $\leq B_x \leq$ 10 nT, $-1.2R_M \leq X \leq -0.75R_M$) and solar EUV flux. It is observed that fluxes of ions with $E > 30$ eV do not depend on solar irradiance while fluxes of ions with lower energy display an obvious increase at high EUV

values. Similar to the observations near the terminator the enhancement of ion fluxes occurs at high solar irradiance. The absence of a EUV-dependence for fluxes of ions with $E > 30$ eV was one of the reasons for separation of ions into high and low energy components. Moreover, such a separation is natural that is confirmed by analysis of ion distribution functions in the Martian tail (*Nilsson et al.,* 2012, *Fraenz et al.,* 2015). Note that the real energy of the low-energy oxygen ions is usually lower since the ions in the tail are additionally accelerated by the spacecraft potential.

Fluxes of low-energy oxygen ions are not axially symmetrical. A strong asymmetry is observed betweeen the hemispheres in which the vector of the solar wind motional electric field is pointed outward from the planet ($+Z_{MSE}$-hemisphere) and inward to the planet ($-Z_{MSE}$-hemisphere). Figure 8 shows maps of fluxes of O_2^+ ions in the $YZ-MSE$ planes at $-1.5R_M \leq X \leq -1R_M$ in the tail. Figure 8a depicts the median fluxes at all levels of solar irradiance. An obvious shift of flows toward the $-Z_{MSE}$ hemisphere is observed. Data shown in Figures 8b and 8c were sorted by the EUV flux. Besides the asymmetry a strong dependence of fluxes in the $-Z_{MSE}$ hemisphere on solar radiation is seen.

4. Discussion

We have performed multi-instrument analysis of the relationship between solar EUV fluxes and processes in the upper ionosphere and escape fluxes of oxygen ions based on the MAVEN observations between November 1, 2014 and February 15, 2016. The response of the ionosphere at altitudes < 250 km to solar activity is not surprising since the bulk of the Martian ionosphere is controlled by the balance between photoionization and recombination. Therefore variations in the density of the main ionospheric peak at the dayside follow well variations in EUV (10-90 nm) flux (*Mendillo et al.,* 2003, 2013,

Breus et al., 2004, *Zou et al.,* 2006). A similar trend is observed in the variations with solar irradiance of the ionospheric column density or total electron content (TEC), which is the electron density integrated over the height (*Lillis et al.,* 2010, *Dubinin et al.,* 2016). At higher altitudes processes of diffusion and transport begin to prevail. The recent observations of the electron number density by the Mars Advanced Radar for Subsurface and Ionospheric Sounding (MARSIS) at altitudes above $\sim$ 300 km on Mars Express (MEX) show that solar irradiance remains to be the controlling factor for the upper ionosphere too (*Dubinin et al.,* 2017). The authors used as a proxy the solar EUV flux at Earth scaled and shifted to Mars.

Since MAVEN carries the Extreme Ultraviolet Monitor measuring solar irradiance in different bandwidths we, for the first time, have an opportunity to compare the simultaneous observations of solar EUV with in-situ ion measurements. The NGIMS observations at altitudes below 500 km near the terminator show that the upper ionosphere surveyed by MAVEN efficiently responds to variations in solar irradiance. With a modest increase of solar EUV flux (factor of 2) the ion density of O_2^+ and O^+ ions in the upper ionosphere (200-300 km) also increases at 1.5-2 times that is a stronger than $\sqrt{EUV}$ dependence expected for lower altitudes. A significant enhancement in ion density is observed at higher altitudes sampled by the STATIC measurements. But in contrast to the MAVEN/MEX observations which show a linear increase in the variables ($logN_e - EUV$) (*Dubinin et al.,* 2017), the MAVEN data exhibit a sudden strong rise at EUV $\geq$ 0.1 W/m^2 with an amplification factor of $\sim$ 10. A similar behavior is observed for the trans-terminator fluxes although at altitudes above $\sim$ 800 km ion fluxes at higher EUV flux decrease and become even less than the corresponding fluxes at high solar irradiance. Probably, at

high altitudes the role of solar wind as a driver becomes more important and we need to separate effects of solar wind and EUV more accurately.

We have also analyzed effects of solar irradiance on losses of oxygen ions through different escape channels. We have considered three main routes of ion escape: 1) ions extracted from the hot oxygen corona and the exterior ionospheric layers and moving on cycloidal trajectories (classical pickup), 2) ions extracted from deeper ionospheric shells which form a 'comet-like' flow pattern, 3) ions accelerated by j x B force in the plasma sheet.

Fluxes carried by pickup ions which mainly occupy the regions outside the induced Martian magnetosphere do not reveal any dependence on solar EUV. We suppose that the main driver for this ion population is the solar wind. Most of the escape flux at the distances surveyed by MAVEN is contained within the magnetosphere although the energy gained by particles in this area is generally smaller than the energy of heavy planetary ions observed in the magnetosheath and solar wind. While fluxes of more energetic ions in the tail are also not sensitive to solar irradiance, fluxes of low-energy ions reveal a strong increase at high EUV. We assume that the ion energization in the tail occurs mainly under the action of the $j \times B$ force which in their turn is determined by the solar wind dynamic pressure. In contrast, low-energy planetary ions are forced, at least partly, by the pressure gradient which should be positively correlated with the EUV flux. A strong enhancement of ion fluxes in the tail occurs at EUV $\geq$ 0.1 W/m^2 when the low energy oxygen ions fill the whole wake and their fluxes exceed 10^7 cm^{-2}s^{-1}. It is difficult to explain such a behavior in terms of a simple balance between photoionization, recombination and ion transport. We can assume, for example, that when the ionosphere becomes denser and

expands upwards the scavenging processes forced by solar wind are strongly enhanced. Note that a strong nonlinear increase of ion escape with EUV is observed in the recent simulations by *Brecht et al.,* (2016)

The MAVEN observations also show a shift of ion fluxes toward the $-Z_{MSE}$-hemisphere. A similar asymmetry was observed in the near Venus tail (*Dubinin et al.,* 2013).

The value of the total losses of the low-energy oxygen component is very sensitive to the geometry of the escape channel. Therefore we need more sampling of the low-energy ion fluxes at the apoapsis area ($\sim 2.3R_m$) at high values of solar irradiance. A conservative estimate of total losses is $L \sim \pi(1.25R_m)^2 \cdot F \cdot k$, where $F \sim 1.6 \cdot 10^6$ cm^{-2}s^{-1} (low EUV); $F \sim 1.6 \cdot 10^7$ cm^{-2}s^{-1} (high EUV) and k is a factor which takes into account fluxes of the molecular and atomic oxygen ions. Taking $k \sim 2$ implies $L \sim 1.8 \cdot 10^{24}$ (low EUV) and $L \sim 1.8 \cdot 10^{25}$ s^{-1}.

The interesting question still remains whether and how fluxes of low-energy oxygen ions are affected by another important driver for losses forced by solar wind - the solar wind dynamic pressure. Figure 9 shows the trans-terminator fluxes of oxygen ions at altitudes of 400-600 km as a function of solar irradiance and solar wind dynamic pressure. The latter was retrieved from the SWIA measurements on the same orbits. Although statistics are rather poor we observe that solar irradiance is the more important factor for losses of the low-energy ions.

Note that the range of variations in EUV power emitted by Sun during MAVEN observations is very restricted, it varies only by a factor of ~ 2.5. In contrast, the solar irradiance in the early epoch was 100-1000 times larger than now (*Ribas et al.,* 2005). We can hardly extrapolate the present observations to such extreme conditions without taking into con-

sideration changes in other global parts of the coupled atmosphere-ionosphere-solar wind systems and therefore modelling efforts would be very timely.

Acknowledgments. Authors ED, MP, wish to acknowledge support from DFG for supporting this work by grant PA 525/14-1. Authors ED and MF wish to acknowledge support from DLR by grant 50QM1302. OV and LZ wish to acknowledge support from the Russian Science Foundation by grant 16-42-01 103. The MAVEN observational data used in the study were obtained from the NASA Planetary Data System (PDS).

References

Barabash, S., A. Fedorov, R. Lundin, and J.-A. Sauvaud (2007), Martian atmospheric erosion rates, *Science, 315(5811), 501-503,* doi:10.1126/ science.1134358.

Brain, D. A., J.P. McFadden, J. S. Halekas et al. (2015), The spatial distribution of planetary ion fluxes near Mars observed by MAVEN, *Geophys. Res. Lett. 42,* doi:10.1002/2015GL065293.

Brecht, S. H., S. A. Ledvina, and S. W. Bougher (2016), Ionospheric loss from Mars as predicted by hybrid particle simulations, *J. Geophys. Res., Space Physics, 121, 10,190-10,208,* doi:10.1002/2016JA022548.

Breus, T. K., A. M. Krymskii, D. H. Crider, et al. (2004), The effect of the solar radiation in the topside atmosphere/ionosphere of Mars: Mars Global Surveyor observations, *J. Geophys. Res., Space Physics, 109, A09310,* doi:10.1029/2004JA010431.

Connerney, J. E. P., J. Espley, P. Lawton et al. (2015), The MAVEN magnetic field investigation, *Space Sci. Rev,* doi:10.1007/s11214-015-0169-4.

Dong, Y., X. Fang, D. A. Brain et al. (2015), Strong plume fuxes at Mars observed by MAVEN: An important planetary ion escape channel, *Geophys. Res. Lett. 42,* doi:10.1002/2015GL065346.

Dong, Y., X. Fang, D. A. Brain et al. (2017), Seasonal variability of Martian ion escape through the plume and tail from MAVEN observations, *J. Geophys. Res., Space Physics, 122,* doi:10.1002/2016JA023517.

Dubinin E., K. Sauer, R. Lundin et al. (1996), Plasma characteristics of the boundary layer in the martian magnetosphere, *J. Geophys. Res., Space Physics, 101, 27061-27075.*

Dubinin, E., M. Fraenz, J. Woch et al. (2006), Plasma morphology at Mars. ASPERA-3 observations, *Space Sci. Rev, 126, 209.*

Dubinin, E., Fraenz, M., Fedorov A. et al. (2011), Ion energization and escape on Mars and Venus, *Space Sci. Rev, 162, 173-211,* doi: 10.1007/s11214-011-9831-7.

Dubinin, E., M. Fraenz, J. Woch et al. (2012), Bursty escape fluxes in plasma sheets of Mars and Venus, *Geophys. Res. Lett. 39,* L01104, doi:10.1029/2011GL049883.

Dubinin, E., M. Fraenz, T. L. Zhang et al. (2013), Plasma in the Near Venus Tail - Venus Express Observations, *J. Geophys. Res., Space Physics, 118,* doi:10.1002/2013JA019164.210.

Dubinin, E. and Fraenz, M. (2015), Magnetotails of Mars and Venus, in *Magnetotails in the Solar System (eds A. Keiling, C. M. Jackman and P. A. Delamere), John Wiley & Sons, Inc, Hoboken, NJ.* doi: 10.1002/9781118842324.ch3.

Dubinin, E., M. Fraenz, D. Andrews, D. Morgan (2016). Martian ionosphere observed by Mars Express. 1. Influence of the crustal magnetic fields, *Planet. Space Sci. 124, 62-75,* http://dx.doi.org/10.1016/j.pss.2016.02.004.

Dubinin, E., M. Fraenz, Pätzold et al. (2017), Martian ionosphere observed by Mars Express. 2. Influence of solar irradiance on upper ionosphere and escape fluxes., *Planet. Space Sci.*

Eparvier F. G., P. C. Chamberlin, T.N. Woods and E. M. B. Thiemann (2015), The Solar Extreme Ultraviolet Monitor for MAVEN, *Space Sci. Rev, 195, 293-301,* doi 10.1007/s11214-015-0195-2.

Fraenz, M., E. Dubinin, E., E. Nielsen et al. (2010), Transterminator ion flow in the Martian ionosphere. *Planet. Space Sci. 58, 1442-1454.* doi:10.1016/j.pss.2010.06.009.

Fraenz, M., E. Dubinin, D. Andrews et al. (2015), Cold ion escape from the Martian ionosphere, *Planet. Space Sci. 119, 15,92-102,* http://dx.doi.org/10.1016/j.pss.2015.07.012.

Halekas, J. S., E. R. Taylor, G. Dalton et al. (2015), The Solar Wind Ion Analyzer for MAVEN, *Space Sci. Rev,* doi:10.1007/s11214-013-0029-z.

Jakosky, B. M., J. M. Grebowsky, J. G. Luhmann et al. (2015a), MAVEN observations of the response of Mars to an interplanetary coronal mass ejection, *Science, 111, A09213,* doi:10.1126/science.aad0210.

Jakosky, B. M., et al. (2015b), The Mars Atmosphere and Volatile EvolutioN (MAVEN) mission, *Space Sci. Rev, 21,* doi:10.1007/s11214-015-0139-x.

Lillis, R.J., et al. (2010), Total electron content in the Mars ionosphere: Temporal studies and dependence on solar EUV flux, *J. Geophys. Res., Space Physics, 115, A11314,* doi:10.1029/2010JA015698.

Lundin, R. et al. (1989), First measurements of the ionospheric plasma escape from Mars, *Nature 341, 609-612,* doi:10.1038/341609a0.

Lundin, R., S. Barabash, M. Holmstrm et al. (2008a), A comet-like escape of ionospheric plasma from Mars, *Geophys. Res. Lett. 35,* L18203, doi:10.1029/2008GL034811.

Lundin, R. et al. (2008b), Solar forcing and planetary ion escape from Mars, *Geophys. Res. Lett. 35,* L09203, doi:10.1029/2007GL032884.

Lundin, R. et al. (2013), Solar cycle effects on the ion escape from Mars, *Geophys. Res. Lett. 40,* 6028-6032, doi:10.1002/2013GL058154.

Mahaffy, P. R., et al. (2015), The neutral gas and ion mass spectrometer on the Mars Atmosphere and Volatile Evolution Mission, *Space Sci. Rev, 185,* doi:10.1007/s11214-11014-10091-11211.

McFadden, J., O. Kortmann, D. Curtis et al. (2015), The MAVEN suprathermal and thermal Ion composition (STATIC) instrument, *Space Sci. Rev, 195, 1 199-256,* doi:10.1007/s11214-015-0175-6.

Mendillo, M., S. Smith, J. Wroten et al. (2003), Simultaneous ionospheric variability on Earth and Mars, *J. Geophys. Res., Space Physics, 108(A12), 1432,* doi:10.1029/2003JA009961.

Mendillo, M., A. G. Marusiak, P. Withers et al. (2013), A new semiempirical model of the peak electron density of the Martian ionosphere, *Geophys. Res. Lett. 40,* 5361-5365, doi:10.1002/2013GL057631.

Modolo, R., G. M. Chanteur, and E. Dubinin (2012), Dynamic Martian magnetosphere: Transient twist induced by a rotation of the IMF, *Geophys. Res. Lett. 39,* L01106, doi:10.1029/2011GL049895.

Nilsson, H. et al. (2010). Ion escape from Mars as a function of solar wind conditions: A statistical study, *Icarus 206, 40-49,* doi:10.1016/j.icarus.2009.03.006

Nilsson, H. et al. (2011), Heavy ion escape from Mars, influence from solar wind conditions and crustal magnetic fields, *Icarus, 215(2), 475-484,* doi:10.1016/j.icarus.2011.08.003.

Nilsson, H., et al. (2012), Ion distributions in the vicinity of Mars: Signatures of heating and acceleration processes, *Earth Planets Space, 64, 135-148,* doi:10.5047/eps.2011.04.011.

Ramstad, R. et al. (2015), The Martian atmospheric ion escape rate dependence on solar wind and solar EUV conditions: I. Seven years of Mars Express observations, *J. Geophys. Res. Planets, 120, 1298-1309,* doi:10.1002/2015JE004816.

Ribas, I., E. F. Guinan, M. Gdel, M. Audard (2005), Evolution of the Solar Activity over Time and Effects on Planetary Atmospheres. I. High-Energy Irradiances (1-1700 A), *Astrophysical Journal, 622, 680-694.*

Vaisberg, O. (1976), Mars-plasma environment, in *Physics of Solar Planetary Environment, ed. by D. J. Williams, AGU, Boulder, pp. 854-873.*

Zou, H., J. S. Wang, and E. Nielsen (2006), Reevaluating the relationship between the Martian ionosphere peak density and the solar radiation, *J. Geophys. Res., Space Physics, 111, A07305,* doi:10.1029/2005JA011580.

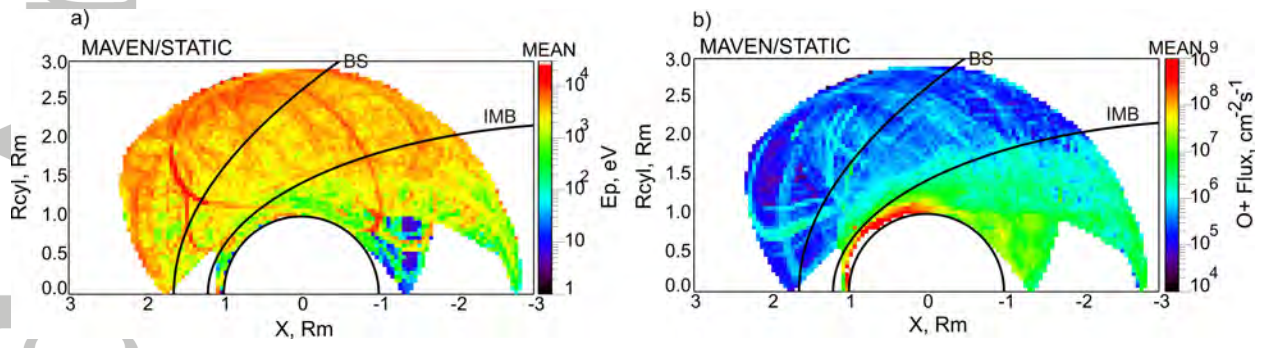

Figure 1. a) Map of the energy of O^+ ions corresponding to the peaks of ion fluxes in cylindrical coordinates. Nominal positions of the bow shock (BS) and the boundary of the Martian magnetosphere (IMB) (*Dubinin et al.,* 2006) are given. b) Map of fluxes of O^+ ions.

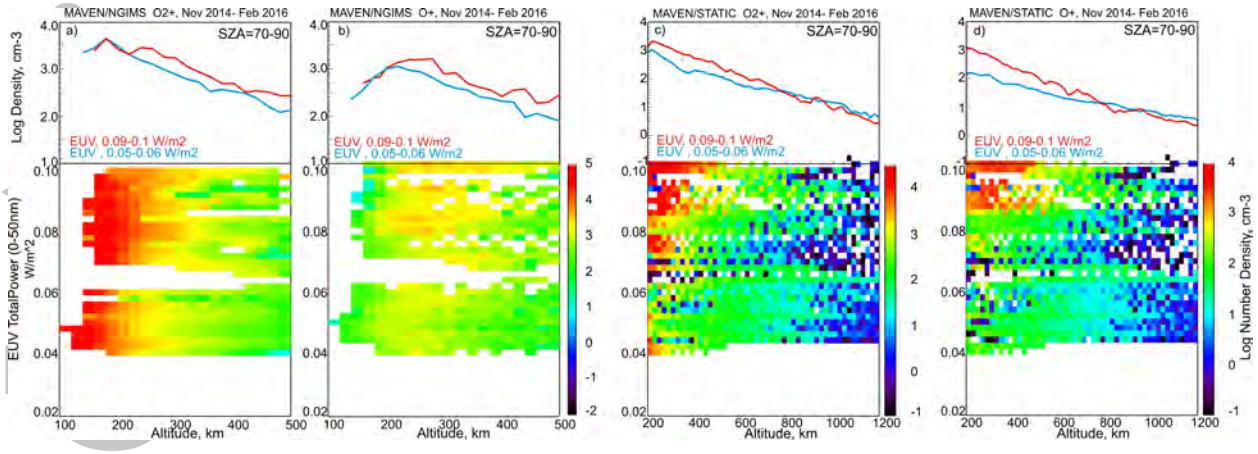

Figure 2. Maps of the density of O_2^+ and O^+ ions measured by NGIMS and STATIC near the terminator (SZA = 70^o-100^o) as functions of altitude and EUV flux. Altitude profiles of the ion densities for two different levels of solar irradiance are shown on the top of the color maps.

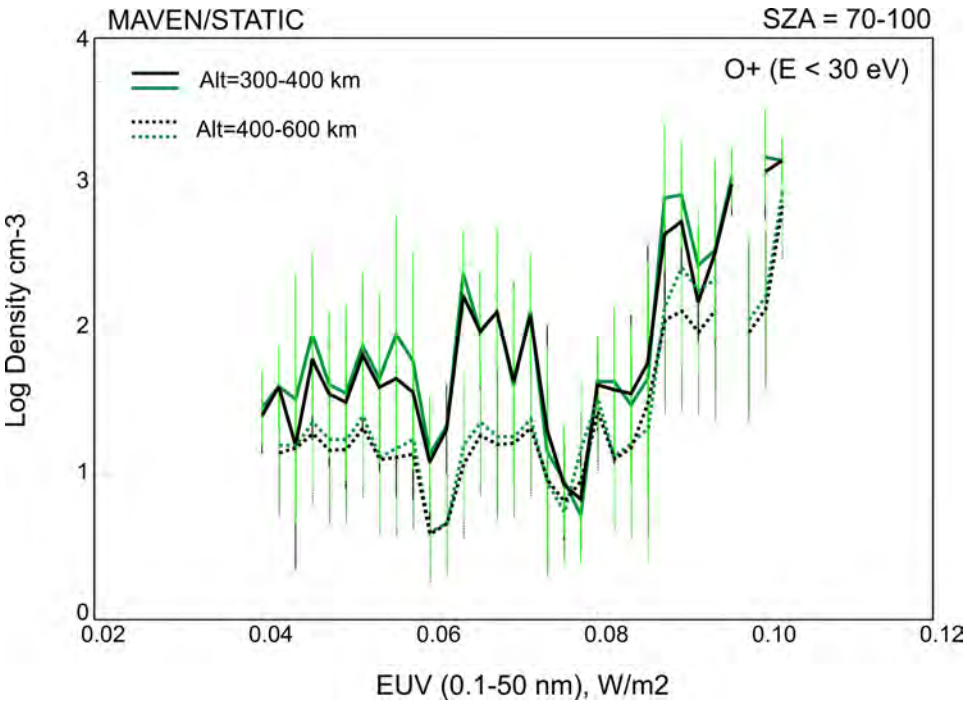

Figure 3. Mean (black) and median (green) values of the density of the oxygen ions with their standard deviations at altitudes of 300-400 and 400-600 km and solar zenith angles $70^o - 100^o$ as a function of EUV flux.

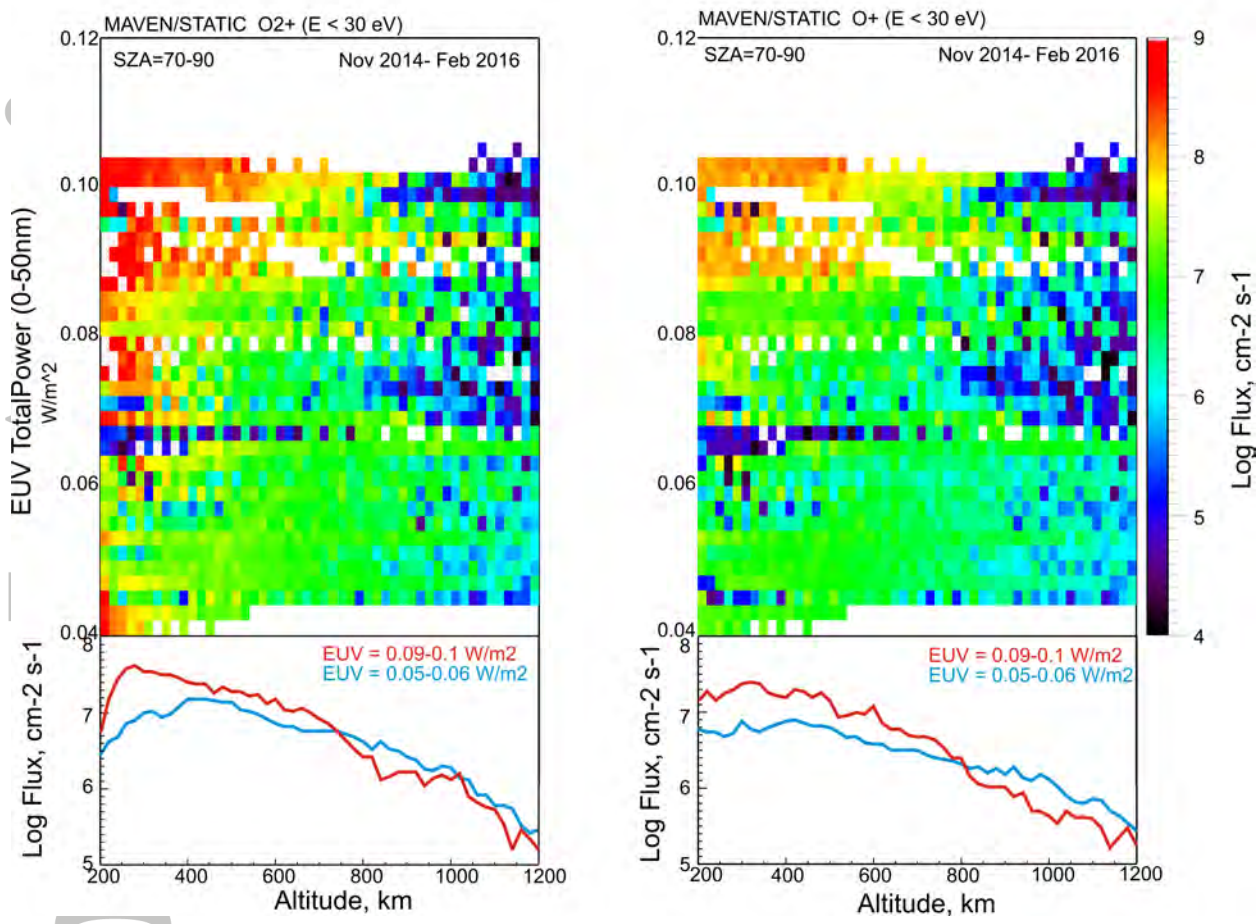

Figure 4. Map of trans-terminator fluxes of O_2^+ and O^+ ions ($E \leq 30$ eV) at different altitudes and different levels of solar activity. Plots on the bottom present the altitude profiles of ion fluxes at two levels of solar irradiance.

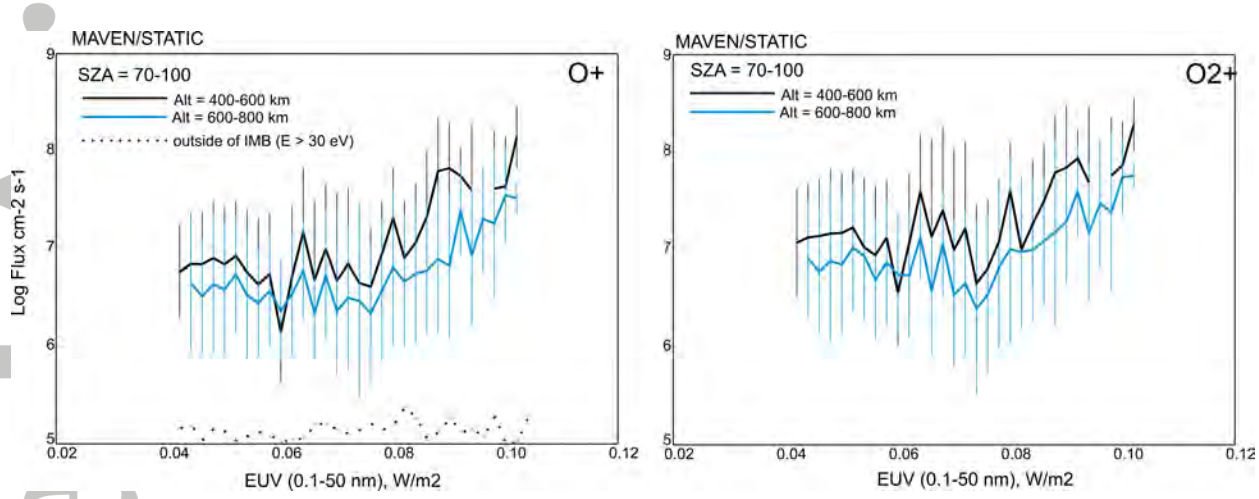

Figure 5. Mean values of trans-terminator fluxes of O^+ and O_2^+ ions ($E \leq 30$ eV) at different altitudes as a function of solar EUV flux. Standard deviations are also given.

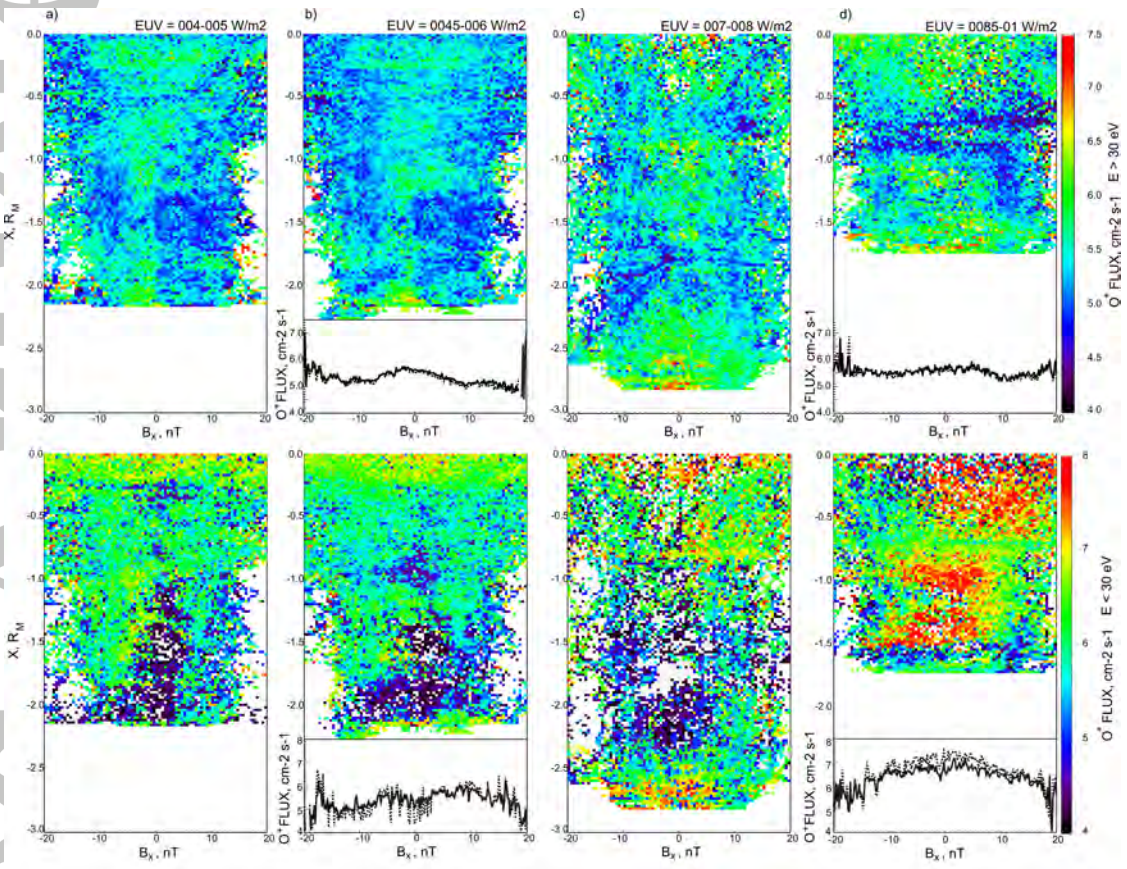

Figure 6. Maps of fluxes of O^+ ions with $E > 30$ eV (upper row) and $E \leq 30$ eV (lower row) in the tail in the $B_x - X$ variables for several different ranges of solar irradiance. Here B_x is the X-component of the local magnetic field, and X - is the X_{MSO} - distance. The current sheet is centered at $X = 0$. The bottom parts of panels (b) and (d) contain the plots of ion fluxes at $-1.6R_m < X < -1.2R_m$ across the tail as a function of B_x for two different states of solar activity - 0.045-0.06 W/m^2 and 0.08-0.1 W/m^2). The solid and dotted lines are the mean and median values, respectively.

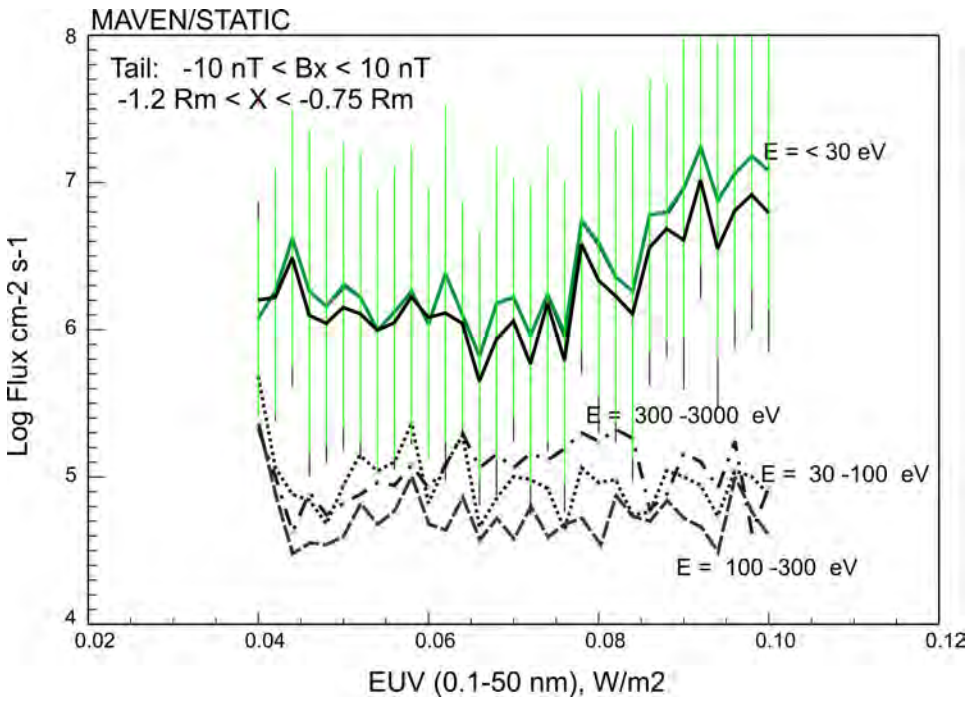

Figure 7. Mean (black) and median (green) values of fluxes of low-energy oxygen ions and their standard deviations in the tail. Mean fluxes of oxygen ions measured in different energy ranges as a function of solar irradiance are also shown.

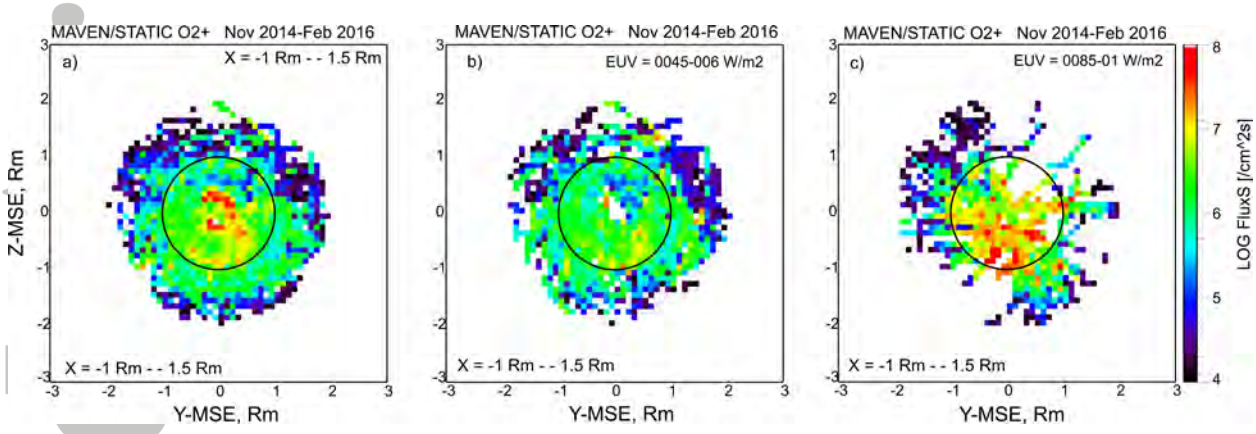

Figure 8. Maps of fluxes of molecular oxygen ions ($E \leq 30$ eV) in the YZ-MSE plane at $-1.5R_M \leq X \leq -1R_M$ for a) all levels of solar activity, b) EUV = 0.045-0.06 W/m^2, c) EUV = 0.085-0.1 W/m^2.

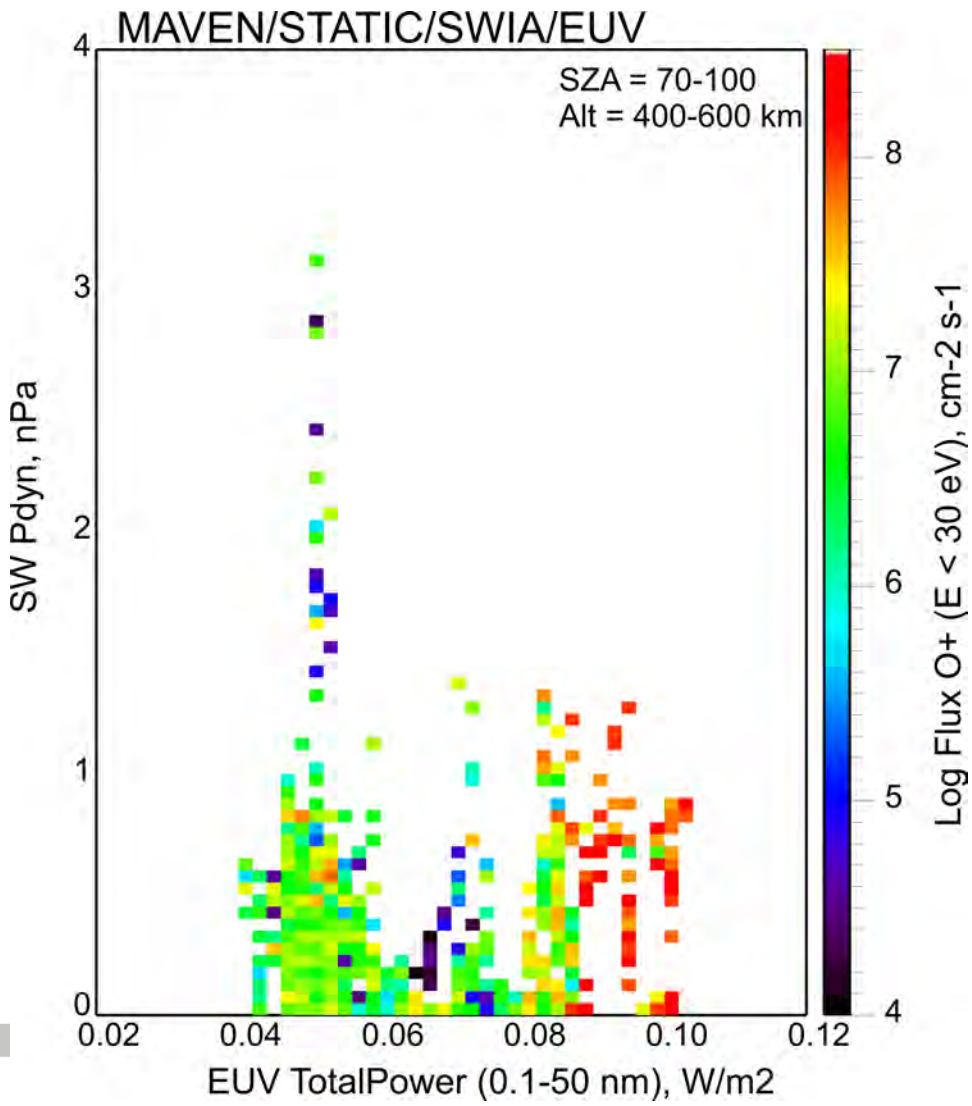

Figure 9. Maps of the trans-terminator fluxes of O^+ ions with $E \leq 30$ eV as a function of solar irradiance and solar wind dynamic pressure.